

Effective stiffening of DNA due to nematic ordering causes DNA molecules packed in phage capsids to preferentially form torus knots

Daniel Reith¹, Peter Cifra², Andrzej Stasiak^{3,*} and Peter Virnau¹

¹Institut für Physik, Johannes Gutenberg-Universität, 55128 Mainz, Germany, ²Polymer Institute, Slovak Academy of Sciences, 845 41 Bratislava, Slovakia and ³Center for Integrative Genomics, University of Lausanne, 1015 Lausanne, Switzerland

Received January 9, 2012; Revised and Accepted January 27, 2012

ABSTRACT

Observation that DNA molecules in bacteriophage capsids preferentially form torus type of knots provided a sensitive gauge to evaluate various models of DNA arrangement in phage heads. Only models resulting in a preponderance of torus knots could be considered as close to reality. Recent studies revealed that experimentally observed enrichment of torus knots can be qualitatively reproduced in numerical simulations that include a potential inducing nematic arrangement of tightly packed DNA molecules within phage capsids. Here, we investigate what aspects of the nematic arrangement are crucial for inducing formation of torus knots. Our results indicate that the effective stiffening of DNA by the nematic arrangement not only promotes knotting in general but is also the decisive factor in promoting formation of DNA torus knots in phage capsids.

INTRODUCTION

Although structures of proteins forming bacteriophage capsids are known with nearly atomic resolution (1–3) the precise arrangement of DNA within the capsids remains to a large extent unknown. Fluidity of tightly packed DNA makes it unsuitable for high-resolution structure determination based on X-ray crystallography or electron microscopy. Although in recent years cryo-electron microscopy studies (4,5) and numerical simulations (6,7) supported models of coaxial and concentric spooling, there is an uncertainty of whether there is a chiral bias in formed spools (8). Such a bias could be caused by axial rotation of DNA during its active loading into the phage capsids (9) or could result from a cholesteric twist angle

induced by steric interactions between highly concentrated right-handed double-helices (10).

When mature bacteriophages such as P2 or P4 are assembled in infected cells their long linear DNA molecules are loaded into phage capsids formed earlier. Each phage capsid receives one linear DNA molecule that is progressively fed starting with its one end through a thin channel that leads through phage tail to the phage capsid, which is the main compartment to store the phage DNA. The loading process, necessitating specialized DNA packaging motors (9), normally stops in such a way that the trailing end of loaded DNA is retained within the phage tail (4,11), that will serve later as the injection needle during the next round of the infection, whereas the rest of the long linear DNA molecule with its leading end is tightly packed within the phage capsid. The two ends of the linear DNA molecules have protruding single stranded extensions that are complementary to each other (12). This complementarity of ends enables rapid circularization of phage DNA upon its injection into a newly infected cell. Such a rapid circularization is crucial for protecting the invading DNA from digestion by bacterial exonucleases. However, in tailless mutants of bacteriophage P4 the lagging end also enters into the phage head during the loading process (13). In this specific situation, the complementary ends can approach each other as a result of thermal motion occurring within the tightly packed but fluid DNA arrangement in the phage capsid. When the two ends meet they anneal with each other so that when the DNA is released from the capsid, using standard laboratory procedures, the DNA ends remain firmly attached (13). Therefore, various types of DNA knots that resulted from DNA arrangement in capsids of bacteriophages maintain their original knot type after DNA isolation and can be investigated by such techniques as electron microscopy (13) and gel electrophoresis (14–16). As DNA

*To whom correspondence should be addressed. Tel: +41 21 692 4282; Fax: +41 21 692 4115; Email: andrzej.stasiak@unil.ch

molecules undergoing cyclization within phage capsids are not distorted by any external force, the formed knot types can provide information about the overall organization of DNA in tightly packed bacteriophage genome.

Studies investigating relative frequencies with which various types of DNA knots formed in bacteriophage capsids revealed that these knots have a much different spectrum as compared to knots formed randomly. For example, while freely fluctuating polymers in free space (17,18) or random trajectories highly confined to a sphere (8) result about twice more frequently in formation of five crossing twist knots (with the standard mathematical notation 5_2) than of five crossing torus knots (5_1) (see Figure 5 for schematic presentations of these knots) the opposite is the case for DNA knots formed in phage capsids (8). The standard mathematical notations of knots such as 5_2 use two numbers where the first one, written with normal fonts, indicates the minimal number of crossings a given knot type can have in a projection whereas the subscript number indicates the tabular position of a given knot type among the knots with the same minimal crossing number in standard tables of knots. Another ‘anomaly’ of knots formed in phage heads concerns the four crossing knot 4_1 (see Figure 5). That type of knots due to its relative simplicity forms much more frequently than five crossing torus knots (5_1) or five crossing twist knots (5_2) by random trajectories in confined volumes (8) or by DNA knots formed in free solution (19,20). However, among knots formed in phage capsids knot 4_1 is found strongly underrepresented and forms significantly less frequently than 5_1 or 5_2 knots (8).

Although the determination of the specific knot spectrum formed by DNA molecules that circularized in tailless phages provided a sensitive signature of DNA arrangement within phage capsids, it is not possible yet to directly interpret this knotting signature in terms of predicting the geometry of DNA arrangements that will result in formation of the same spectrum of DNA knots. The researchers in the field rather use a trial and error method where they test different models by simulations and analyse what type of knots would result from a given model. So, for example, Marenduzzo *et al.* (21,22) have shown recently that numerical simulations incorporating a potential inducing a nematic arrangement of tightly packed DNA molecules produced a very similar spectrum of knots to the one observed in real DNA molecules that were circularized within bacteriophage capsids. Marenduzzo *et al.* assumed that the cholesteric twist angle between sequential layers of nematically arranged segments of the same long DNA molecules can be responsible for the observed preponderance of chiral knots. To test this hypothesis, they have compared models where the cholesteric twist angle was set to 1° , which is in the upper range of the cholesteric twist angle values observed in DNA liquid crystals (23), with models where the nematic potential was not inducing any cholesteric twist. Interestingly, the two conditions produced nearly identical spectra of knots. This result indicates that the cholesteric twist, which most likely is present in the nematic arrangement of tightly packed DNA in bacteriophage capsids, is

not essential for the observed preponderance of torus knots in DNA molecules circularized within phage capsids.

What is then the decisive factor in nematic DNA arrangements that can favour formation of torus knots in tightly packed DNA? Nematic arrangement in addition to imposing a correlation between directions of DNA segments that approach each other laterally also induces a correlation between consecutive segments of the same molecule, where this correlation effectively increases the persistence length of DNA molecules (24). To test whether it is the effective stiffening of DNA that causes preferential formation of torus knots in phage capsids, we used numerical simulations to investigate how changes of polymer stiffness affect knotting of modelled semiflexible polymers strongly confined within a sphere.

MATERIALS AND METHODS

Coarse-grained polymer model

A bead-spring model based on (25) was used to model the polymer chain. In this model, the interaction between non-bonded monomers is modelled by a purely repulsive cut and shifted Morse potential:

$$U_{\text{MORSE}}/\varepsilon = \begin{cases} \exp[-48(x-0.8)] - 2 \exp[-24(x-0.8)] + 1 & \text{if } x < 0.8 \\ 0 & \text{else} \end{cases}$$

The parameters of the model were chosen to allow comparison with previous studies (26). The standard simulation unit for length is σ . At 0.8σ , the interactions between non-adjacent beads as defined by our (repulsive) Morse potential become 0. Hence, we regard this value as the diameter of our beads. To convert to experimental units, we set this value equal to 2.5 nm, which is the accepted diameter of DNA at high salt conditions. Taking this conversion into account, one obtains $\sigma = 3.125$ nm.

Consecutive bonded beads are connected with FENE potential:

$$U_{\text{FENE}} = -1.8 \ln \left[1 - \left(\frac{x - 0.7}{0.3} \right)^2 \right]$$

Using this potential, we obtain a typical distance of $\sim 0.73\sigma$ between consecutive bonded beads.

Bending rigidity is introduced by:

$$U_{\text{BOND}}(\alpha) = Bk_B T(1 + \cos[\alpha]),$$

where α is the angle between two successive bonds. (In the following $k_B T = 1$ and $\varepsilon = 1$, which corresponds to good solvent conditions.) A single polymer chain with $N = 200$ segments (of bead diameter 0.8σ and average bond length of $\sim 0.73\sigma$) is confined to a sphere of radius $R_{\text{sphere}} = 5.96\sigma$. This particular value was chosen as it permits to have practically the same ratio between the diameter of the enclosing sphere and the diameter of modelled polymer chains as the ratio between the inner

diameter of phage capsids and the diameter of enclosed DNA (8).

Two types of chains are investigated: The first type is anchored at the surface of the enclosing sphere – similar to viral DNA attached to the loading channel of the capsid. The other type is allowed to move freely within the sphere. In combination with local Monte Carlo moves, we apply the slithering snake algorithm (27) for unanchored and end-bridging moves for anchored chains (28) to ensure efficient sampling of topology. The sphere is modelled by an excluded volume interaction, i.e. trial configurations outside the sphere are rejected automatically. For each value of the bending rigidity B , up to 100 independent runs from different starting configurations were used in the analysis. We monitored the average unknotting probability of independent configurations over time and estimated correlation times between unknotted configurations in single runs to ensure that the simulation runs are sufficiently long and the equilibrium distribution is reached. Error bars in Figure 2 refer to the standard error of the mean of the independent runs. Note that our computations are quite expensive and ~20 CPU core years were invested in this study.

Knot identification

Configurations are analysed by applying the following statistical closure (29): We randomly choose two points on a sphere, which is much larger than the polymer, but has the same centre of mass. Then, these two points are connected by a line with each other and one of the points is connected by a line with the first monomer of the chain while the second point is connected with the last monomer of the chain. The resulting closed curve is classified topologically by computing the Alexander polynomial (30). The whole procedure is repeated 100 times for each configuration and the knot is defined as the majority type. Although the Alexander polynomial does not distinguish between right- and left-handed forms of chiral knots this distinction is not required since the generic polymer model applied by us does not break the symmetry and therefore right- and left-handed forms of chiral knots are expected to form with the same frequencies.

RESULTS

To investigate how polymer stiffness affects the spectrum of knots resulting from cyclization of polymers in a spherical confinement, we performed Monte Carlo simulations that produced equilibrated statistical ensembles of long linear polymer chains with different stiffness but subject to the same spherical confinement. Our chains were simulated using a specific bead spring model where consecutive beads in a chain could partially interpenetrate (31) (for more details, see ‘Materials and Methods’ section). The chains were composed of 200 beads, whereas the radius of the confining sphere was set to 7.45 bead diameters. This number roughly corresponds to the ratio between the inner radius of P4 capsid and the effective diameter of DNA at high salt conditions (8). Assuming that the diameter of beads corresponds to

2.5 nm and taking into account that consecutive beads partially interpenetrate (bond length between adjacent beads is roughly 0.91 bead diameters) the contour length of the modelled chain corresponds to ~455 nm, which is 3.5 times shorter than DNA used to study knotting in phage capsids (32). This shorter length has two important advantages: Firstly, it decreases the concentration of the modelled polymers inside the sphere of confinement and thus does not induce the isotropic/nematic transition, which causes an effective increase of polymer stiffness (24). Secondly, smaller polymer sizes allowed us to explore their available configuration space in a reasonable simulation time.

Our simulations investigated two types of situations. In the first one, the simulated polymer chains had one of their ends anchored at the surface of the enclosing sphere, which would correspond to the situation in wild-type phages where one end of the linear DNA stays in the loading channel. In the second situation, the entire chain could move freely within the sphere, as it is presumably the case for DNA in tailless phage mutants. Equilibrium configurations of chains belonging to these two different situations did not show systematic statistical differences in their shapes and in the spectrum of formed knots when their stiffness was the same. To characterize the knot spectrum that would have resulted from the cyclization of the equilibrated configurations of modelled polymer chains, we utilized a stochastic, unbiased closure method (29). The chain stiffness was controlled in our simulations by changing the value of a parameter B (see Methods section for a more precise description), where the higher the B value the higher the stiffness and where the B value of about 20 makes our model to reproduce the statistical behaviour of DNA molecules.

Chain stiffness stimulates knotting

Figure 1 shows overall shapes adopted by polymers with the same length but different stiffness when confined within a small sphere of the same diameter. We can see that highly flexible polymers fill the sphere of confinement in a rather uniform way (Figure 1A). However, as the stiffness of polymers increases they move toward the periphery of the sphere (Figure 1C and D). This result agrees with the intuitive expectation and an experiment that one could do in the lab by progressively feeding into a spherical distillation flask a long cotton string or a relatively stiff wire.

A somewhat unexpected result was obtained, though, when we investigated how the frequency of knotting changes with the stiffness of modelled chains. It is known that in a free space knotting of polymers increases with the number of statistical segments in a chain (33–35). Therefore, if two polymers have the same physical length and the same effective diameter the more flexible will be more knotted than the less flexible one. However, we observed the opposite trend for polymers confined to a restricted volume. Whereas the highly flexible polymers were hardly knotted the frequency of knots has risen to >80% as the stiffness of polymers was increased (see insets in Figure 2).

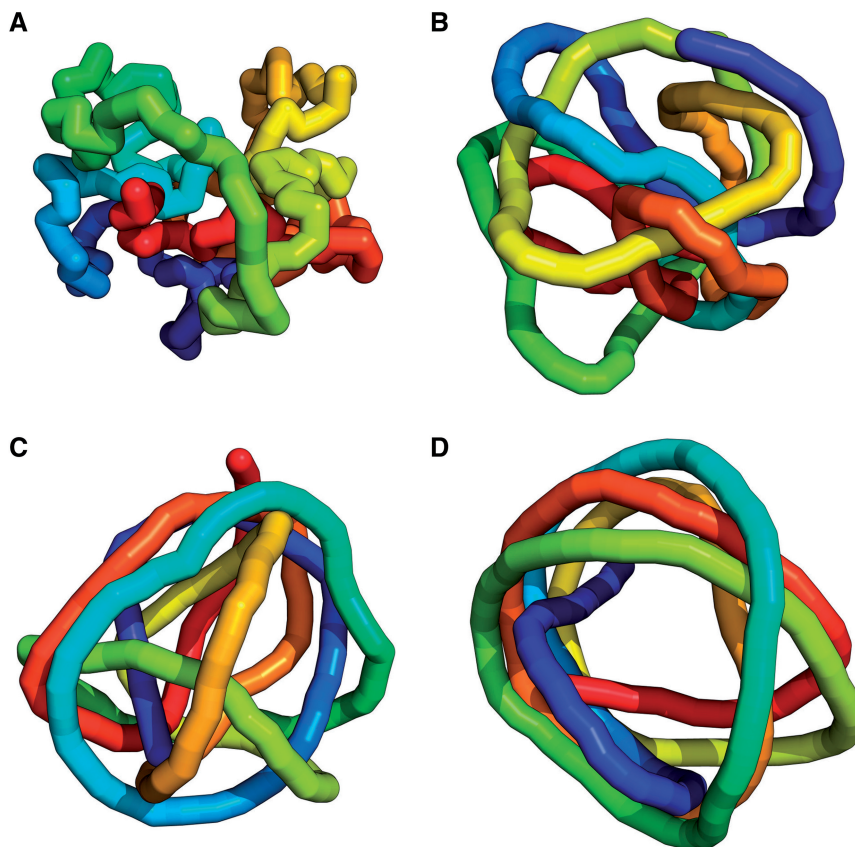


Figure 1. Effect of increasing stiffness on the overall shapes of polymer chains having the same length and being confined within a small sphere of the same diameter. (A) In case of fully flexible chains ($B = 0$), equilibrated configurations fill the available volume in a rather uniform way. (B), (C) and (D) present representative snapshots of polymer chains with increasing stiffness and having values of the parameter B amounting to 10, 20 and 45, respectively. Notice that as chains get stiffer they progressively adopt spool-like configurations with the centre being unoccupied. Whereas the configuration shown in (A) is unknotted, the remaining configurations are knotted. All snapshots show unanchored chains but anchored chains have very similar overall appearance.

Spectrum of knots changes with increasing stiffness

Seeing that increasing stiffness of confined polymers leads to their increased tendency to form knots, we decided to analyse the types of formed knots. We were especially interested in investigating whether the increased stiffness can result in producing a spectrum of knots with characteristics known for the DNA knots produced in phage capsids. As compared to DNA knots expected to form in non-confined situation, DNA knots formed in phage capsids showed a predominance of torus knots over twist knots and also showed a strongly reduced frequency of achiral 4_1 knots (8).

Figure 2 in addition to presenting the effect of polymer stiffness on the overall extent of knotting (see insets) also shows how the relative frequency of various formed knots changes as a function of chain stiffness. While maximally flexible polymers composed of 200 segments formed so few knots that their statistics was not reliable, polymer chains with a stiffness that would correspond to 4 times lower persistence length than this of DNA ($B = 5$) formed a spectrum of knots which is typical for knots formed in unconfined polymers. The twist knots 5_2 were roughly twice more frequent than torus knots 5_1 whereas knots 4_1 were more frequent than each of five crossing knots (18). However, as the stiffness of modelled polymers

increased the torus knots 5_1 were formed more frequently than the twist knots 5_2 and the frequency of 4_1 knots decreased below the frequencies of individual five crossings knots, while 3_1 knot remained the dominant knot type. Therefore, as the stiffness of modelled polymers confined into a sphere is increased the spectrum of knots progressively shifts from this characteristic spectrum for unconfined polymers to a spectrum characteristic for DNA knots formed in phage capsids. As shown in Figure 2A and B, non-anchored and anchored modelled polymers behave essentially in the same way with respect to frequency of formed knots.

It needs to be said here that for computational reasons our modelled DNA chains are more than three times shorter than DNA molecules circularized in phage capsids (32). Therefore, we should not expect our simulated knotting spectrum to correspond to the one observed experimentally (32). The best we can expect is to reproduce the trend, i.e. observe stimulation of formation of torus knots and observe relative suppression of 4_1 knots.

Formed entanglements are delocalized

In wild-type phages, the two complementary ends do not meet in the capsid and thus the entanglements do not

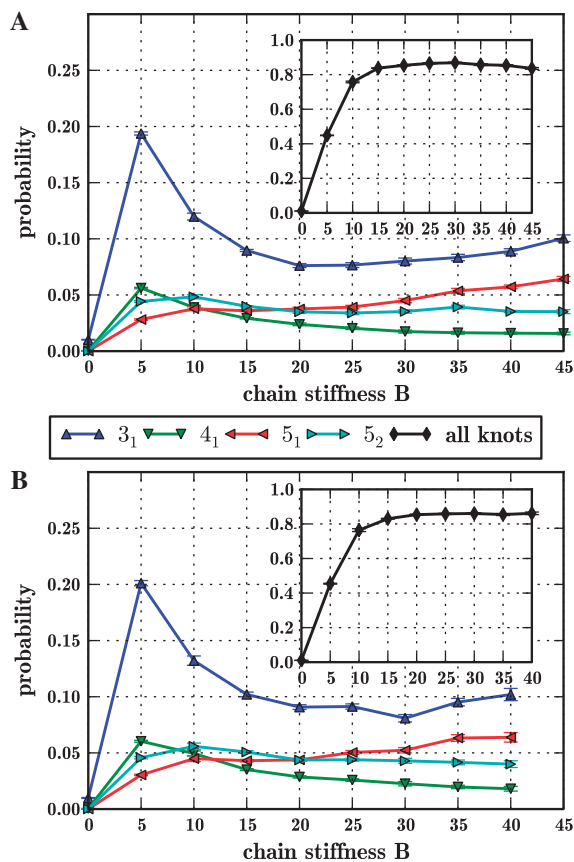


Figure 2. Effect of increasing stiffness on the probability of knotting of polymer chains that are about 12 times longer than the diameter of the confining sphere. Notice that the initial increase of stiffness greatly increases the overall probability of knotting (shown in insets), whereas a further increase of stiffness only changes the relative ratios between formed knots of various types. The characteristic ratio between different knot types observed for modelled polymers with high stiffness resembles the corresponding ratios in DNA knots formed in phage capsids (8). (A) and (B) show the knotting probability profiles for modelled polymer chains that had two or one free ends, respectively. Straight lines are guides to the eyes.

become topologically fixed. However, entanglements may become an obstacle if formed knots could get tightened on the DNA and thus interfere with DNA ejection through a thin channel passing through phage tail (36). Although, it is intuitively expected that increasing stiffness should decrease the chance of having tight knots, we decided to investigate what is the effect of increasing stiffness on the size of the knotted portion of the chain.

To investigate how polymer stiffness affects the spatial extent of knotted portions of the simulated chains, we concentrated on polymer chains that formed 3_1 knots upon unbiased closure and delimited then knot cores of individual configurations, i.e. the portion of the chain that is responsible for formation of 3_1 knot by the entire chain. Searching for the borders of knots' cores we followed the approach of References (37–39) by treating the analysed configurations as frozen and removing progressively monomers first from one end until the remaining chain was still forming the original knot type and then the chain was further trimmed from the other end using the

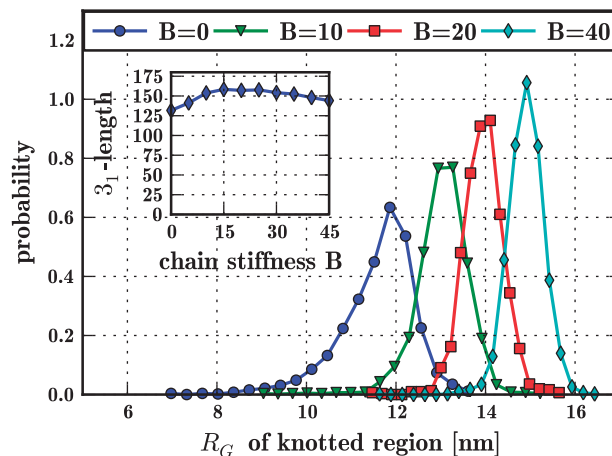


Figure 3. Increasing stiffness decompactifies knotted portions of confined (unanchored) polymer chains. Probability distribution functions of radii of gyration are calculated for knotted portions of polymer chains forming 3_1 knots. Values of radii of gyration are expressed in nm by setting the diameter of modelled chains to 2.5 nm as this is the accepted diameter of DNA when it is packed within phage capsids (21). Inset: Number of segments occupied by the knot in trefoil knotted chains (of total size $N = 200$) as a function of stiffness. For all B , knots are delocalized. Straight lines are guides to the eyes.

same criteria. Subsequently, we measured radii of gyration of knots' cores. Figure 3 shows probability distribution functions of radii of gyration of 3_1 cores in polymer chains with different stiffness. It is very well visible that increasing stiffness increases spatial extent of knotted portions, even if the actual length of knotted portions is hardly affected as in each case knots tend to occupy large sections of the whole chain (inset) and are thus delocalized. Therefore, despite the fact that increasing stiffness increases the probability of knot formation by the confined polymers, the formed knots are in fact becoming less compact than knots formed on flexible polymers. Translating this phenomenon to the case of DNA packed in phage capsids, we can conclude that increasing stiffness decreases formation of tightened knotted domains and thus facilitates DNA ejection during phage infection. Therefore, one could expect that biological systems such as phages evolved in such a way that permits the packed DNA to increase its effective stiffness and we will discuss how this is achieved.

DISCUSSION

Our simulations revealed that stiffening of polymers confined to a small sphere naturally leads to their increased probability of knotting with marked predominance of torus types of knots. This observation can be surprising when one takes into account that in free space a more stiff polymer is less likely to form knots than a less stiff polymer with the same physical length as the knotting probability increases with the number of statistical segments in unconfined polymers (33–35).

Can we understand why more stiff polymers are more likely to form knots upon confinement? In a general sense, to form a knot an individual polymer chain has to thread

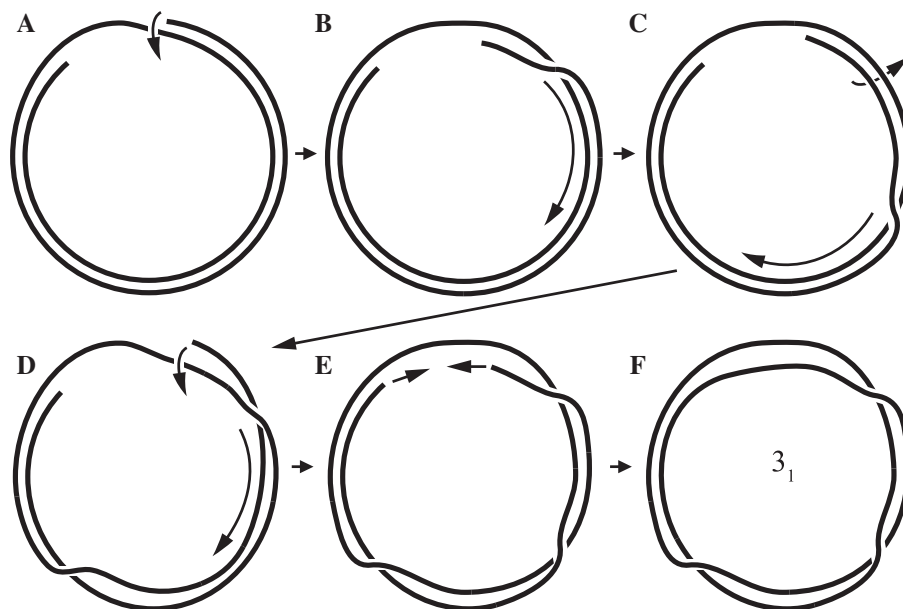


Figure 4. Threading events involving neighbouring loops in coaxially spooled polymer chain lead to entanglement that can cause polymer knotting when the two ends anneal. (A–E) random threading events, (E–F) ends' annealing.

through a loop formed by another portion of the same polymer chain. The probability of passing through formed loops increases with the projected area of these loops. In case of very flexible polymers confined to a sphere such as illustrated in Figure 1A, the formed loops are usually small and therefore the probability of threading through them by other parts of the polymer is low. Stiff polymers confined to a sphere with the diameter smaller than the persistence length of the polymer naturally form very large loops with spool character (26). The neighbouring loops fluctuate and if one of them contains the free end of the polymer this end can easily thread through the neighbouring loop (see Figure 4A and B). The portions of two loops can swap their places with time (Figure 4C) and after some more time the free end can start another threading event, which could, e.g. return it to its original position by completing the rotation around the polymer chain forming the neighbouring loop (Figure 4D) or by reversing the half-turn rotation. Even in the absence of any bias favouring right- or left-handed winding of neighbouring loops, one should expect that after many such threading events the polymer will acquire several entanglements that will lead to formation of knots upon joining of polymer ends. The knotting equilibrium level will depend on the capacity of neighbouring loops to wrap around each other and this eventually decreases as the loops become very stiff (see Figure 2). A sequence of threading events that can lead to creation of a 3_1 knot is shown in Figure 4, while more complex sequences of threading events involving two and more neighbouring loops can lead to formation of more complex knots.

Can we understand why stiff polymers confined into a sphere form preferentially 5_1 torus knots over 5_2 twist knots while the contrary is the case for very flexible

polymers? At least a part of the answer is provided by the fact that stiff polymers within the sphere of confinement adopt trajectories without inflection points and while such an arrangement is natural for torus knots it is rather atypical for twist knots. Although a 5_2 twist knot can be formed by an inflection free 'toroidal' trajectory (40), this trajectory requires involvement of three consecutive coaxial loops and needs to have a complex pattern of interweaving involving all three coaxial loops and necessitating six crossings with a specific combination of signs and also of under and over passages (see Figure 5). A 5_1 torus knot, in turn, in its typical toroidal form only needs to involve two consecutive coaxial loops and necessitates a simpler pattern of interweaving with just five crossings between the two loops (see Figure 5). Taking the above elements into account, it seems natural to expect that restriction of permitted configurations to 'toroidal', inflection-free configurations entails that such configurations will more frequently result in formation of torus type 5_1 knots than twist type 5_2 knots.

Can we understand why 4_1 knots form less frequently than 5_1 or 5_2 knots in case of configurations without the inflection points (37) whereas the opposite is the case for configurations that can populate the entire configuration space (17–20,41)? Similarly to the case of 5_2 knot the 4_1 knot belongs to the twist family of knots and its standard tabular representation contains two inflection points (see Figure 5). It is possible though to form 4_1 knots starting from a 'toroidal' inflection-free configuration (40) but this requires placing in a convenient proximity three consecutive coaxial loops (see Figure 5). Therefore, the overall arrangement preconditioning the possibility of forming a 4_1 knot is quite complex and resembles the requirements for the formation of a 5_2 knot. Although formation of a 4_1 knot requires only four 'interweavings' with a specific

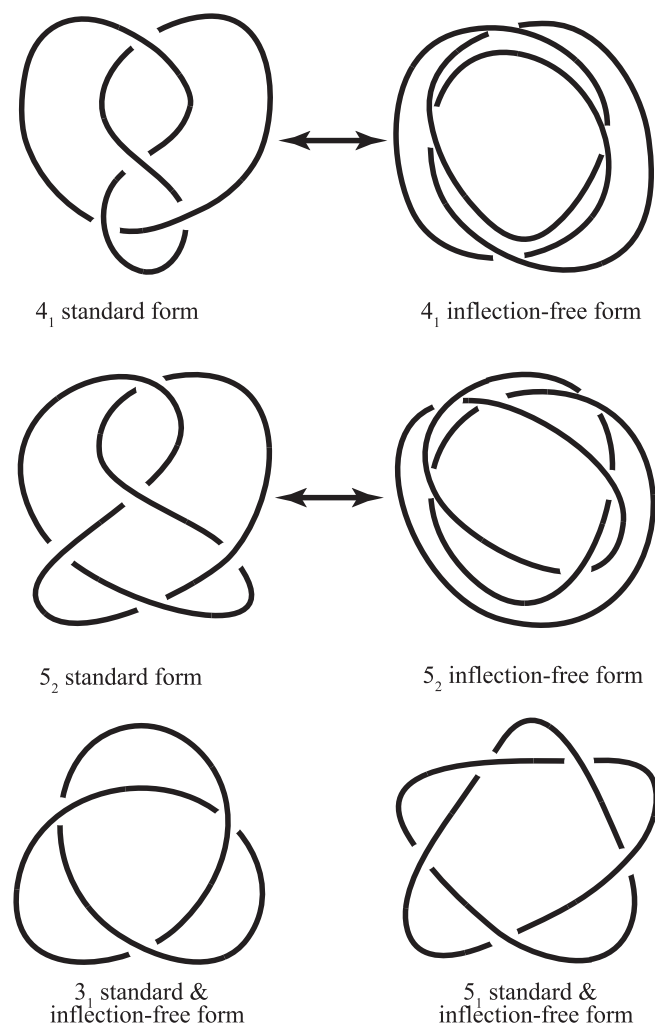


Figure 5. Coaxially spooled inflection-free configurations are more difficult to attain for twist knots such as 4_1 and 5_2 than for torus knots such as 3_1 and 5_1 .

sequence of right- and left-handed crossings and under and over passages and therefore in principle achieving this pattern may be simpler than the specific pattern needed to form 5_2 knots with six 'interweavings'. However, the 5_2 knot is chiral and exists in two enantiomeric forms and therefore there are two different minimal 'interweavings' patterns that produce 5_2 knots while there is only one minimal 'interweaving' pattern that leads to formation of achiral 4_1 knots. The above explanation is probably not complete as we considered only minimal interweaving patterns leading to formation of 5_2 and 4_1 knots, whereas there are many other patterns that will permit 'toroidal' configurations to form 5_2 and 4_1 knots, where some will involve nugatory crossings etc. However, we believe that restricting the available configurational space to 'toroidal' or rather coaxial spool configurations is the main factor that causes that in case of DNA circularized within phage capsids the 4_1 knots are less frequent than 5_1 or 5_2 knots.

The points discussed above help us to understand why equilibrated modelled stiff polymers under spherical

confinement produce the spectrum of knots with the characteristics known for DNA knots formed in phage capsids. However, why do our simulations in which we modelled polymer chains with DNA stiffness ($B = 20$) confined to a sphere with the size corresponding to the size of bacteriophage capsids produce a spectrum of knots that was intermediate between the one known from phage capsids and the one modelled using very flexible polymers? Our simulations seem to suggest that the intrinsic stiffness of DNA is not sufficient to result in the domination of 5_1 knots over 5_2 knots and just suffices to make their probability of formation nearly equal (Figure 3). Therefore, one is led to conclude that the effective stiffness of DNA in phage capsids is larger than the stiffness of unconfined DNA. Indeed, this is most likely the case. As already mentioned, while introducing our model, we simulated significantly shorter DNA molecules than phage DNA to avoid crowding that would induce Onsager's isotropic/nematic transition. When the DNA is crowded, as it is the case in phage capsids, it spontaneously undergoes isotropic/nematic transition leading to the appearance of a liquid crystalline phase. In this phase, due to an ordering effect involving many laterally aligned DNA segments each segment is effectively stiffened whereas its intrinsic mechanical rigidity is unchanged (24). This effective stiffening of DNA most likely explains why in our simulations performed in the concentration regime where nematic ordering was not yet induced, we had to stiffen our modelled polymers well above the intrinsic stiffness of DNA to be able to reproduce the main characteristics of the knot spectrum formed by DNA molecules whose ends could anneal within phage capsids.

Our observation that effective stiffening of DNA due to nematic ordering is instrumental in producing the characteristic spectrum of DNA knots in phage particles is in agreement with a recent simulations study of Marenduzzo *et al.* (21) who also invoked a need for nematic arrangement to reproduce knotting characteristics known from biochemical characterization of DNA knots produced in phage particles. However, whereas Marenduzzo *et al.* (21) were suggesting that it is the nematic twist angle known for cholesteric phase of DNA liquid crystals that favours formation of torus knots and disfavors formation of achiral knots, we show here that the mere stiffening of DNA due to nematic arrangement is sufficient to explain why torus knots are favoured during DNA knot formation in phage particles.

In an earlier study aimed to understand the underlying physical principles responsible for the characteristic spectrum of DNA knots formed in phage particles, Arsuaga and Diao (42) analysed knots formed by a subset of equilateral random walks forming spool-like inflection-free configurations. The studied equilateral random walks had no thickness and segments were phantom with respect to each other. The analysis of formed knots in this somewhat abstract model of DNA packing in a phage capsids revealed though that 5_1 torus knots were just slightly more frequent than 5_2 twist knot and that 4_1 knot was less frequent than 5_1 or 5_2 knots and therefore this simple system was close to reproducing the spectrum of knots formed in bacteriophage capsids.

The authors concluded that their model partially describes the situations occurring within phage capsids. We agree with this conclusion and show here that stiffening of DNA such as induced due to formation of nematic arrangement ensures that DNA in phage capsids adopts preferentially spool-like inflection-free configurations. Such a DNA arrangement, in turn, favours formation of torus type of knots when two ends of packed phage DNA anneal with each other.

Several earlier studies proposed that low occurrence of achiral knots 4_1 among the DNA knots formed in phage capsids can be explained by symmetry breaking mechanisms such as DNA writhe induced during DNA loading (8) or a preferential cholesteric twist angle between interacting DNA segments (21). We show here, however, that such symmetry breaking mechanisms are not needed and that observed suppression of achiral 4_1 knots can simply result from effective stiffening of DNA due to nematic ordering of tightly packed DNA. The effective stiffening, in turn, causes the DNA to adopt geometry of coaxial spools and this geometry is not favourable for formation of twist type of knots such as knot 4_1 .

ACKNOWLEDGEMENTS

We gratefully acknowledge computing time at the JSC Jülich and the ZDV Mainz. P.V. would like to acknowledge fruitful discussions with C. Micheletti, K. Binder and K. Landfester.

FUNDING

Swiss National Science Foundation (31003A_138367 to A.S.); Deutsche Forschungsgemeinschaft (SFB 625–A17 to P.V. and D.R.) and Slovak Republic Scientific Grant Agency (VEGA) (2/0144/09 and 2/0093/12 to P.C.). The open access publication charge for this paper has been waived by Oxford University Press - *NAR* Editorial Board members are entitled to one free paper per year in recognition of their work on behalf of the journal.

Conflict of interest statement. None declared.

REFERENCES

- Wikoff, W.R., Liljas, L., Duda, R.L., Tsuruta, H., Hendrix, R.W. and Johnson, J.E. (2000) Topologically linked protein rings in the bacteriophage HK97 capsid. *Science*, **289**, 2129–2133.
- Martín, C.S., Burnett, R.M., de Haas, F., Heinkel, R., Rutten, T., Fuller, S.D., Butcher, S.J. and Bamford, D.H. (2001) Combined EM/X-ray imaging yields a quasi-atomic model of the adenovirus-related bacteriophage PRD1 and shows key capsid and membrane interactions. *Structure*, **9**, 917–930.
- Morais, M.C., Choi, K.H., Koti, J.S., Chipman, P.R., Anderson, D.L. and Rossmann, M.G. (2005) Conservation of the capsid structure in tailed dsDNA bacteriophages: the pseudoatomic structure of phi29. *Mol. Cell*, **18**, 149–159.
- Jiang, W., Chang, J., Jakana, J., Weigele, P., King, J. and Chiu, W. (2006) Structure of epsilon15 bacteriophage reveals genome organization and DNA packaging/injection apparatus. *Nature*, **439**, 612–616.
- Comolli, L.R., Spakowitz, A.J., Siegerist, C.E., Jardine, P.J., Grimes, S., Anderson, D.L., Bustamante, C. and Downing, K.H. (2008) Three-dimensional architecture of the bacteriophage phi29 packaged genome and elucidation of its packaging process. *Virology*, **371**, 267–277.
- Arsuaga, J., Tan, R.K., Vazquez, M., Sumners, D.W. and Harvey, S.C. (2002) Investigation of viral DNA packaging using molecular mechanics models. *Biophys. Chem.*, **101–102**, 475–484.
- Petrov, A.S., Boz, M.B. and Harvey, S.C. (2007) The conformation of double-stranded DNA inside bacteriophages depends on capsid size and shape. *J. Struct. Biol.*, **160**, 241–248.
- Arsuaga, J., Vazquez, M., McGuirk, P., Trigueros, S., Sumners, D. and Roca, J. (2005) DNA knots reveal a chiral organization of DNA in phage capsids. *Proc. Natl Acad. Sci. USA*, **102**, 9165–9169.
- Yu, J., Moffitt, J., Hetherington, C.L., Bustamante, C. and Oster, G. (2010) Mechanochemistry of a viral DNA packaging motor. *J. Mol. Biol.*, **400**, 186–203.
- Kornyshev, A.A. and Leikin, S. (2000) Twist in chiral interaction between biological helices. *Phys. Rev. Lett.*, **84**, 2537–2540.
- Chattoraj, D.K. and Inman, R.B. (1974) Location of DNA ends in P2, 186, P4 and lambda bacteriophage heads. *J. Mol. Biol.*, **87**, 11–22.
- Wang, J.C., Martin, K.V. and Calendar, R. (1973) On the sequence similarity of the cohesive ends of coliphage P4, P2, and 186 deoxyribonucleic acid. *Biochemistry*, **12**, 2119–2123.
- Liu, L.F., Perkocha, L., Calendar, R. and Wang, J.C. (1981) Knotted DNA from bacteriophage capsids. *Proc. Natl Acad. Sci. USA*, **78**, 5498–5502.
- Vologodskii, A.V., Crisona, N.J., Laurie, B., Pieranski, P., Katritch, V., Dubochet, J. and Stasiak, A. (1998) Sedimentation and electrophoretic migration of DNA knots and catenanes. *J. Mol. Biol.*, **278**, 1–3.
- Trigueros, S., Arsuaga, J., Vazquez, M.E., Sumners, D.W. and Roca, J. (2001) Novel display of knotted DNA molecules by two-dimensional gel electrophoresis. *Nucleic Acids Res.*, **29**, E67–E67.
- Arsuaga, J., Vázquez, M., Trigueros, S., Sumners, D. and Roca, J. (2002) Knotting probability of DNA molecules confined in restricted volumes: DNA knotting in phage capsids. *Proc. Natl Acad. Sci. USA*, **99**, 5373–5377.
- Tsurusaki, K. and Deguchi, T. (1995) Fractions of particular knots in Gaussian random polygons. *J. Phys. Soc. Jpn.*, **64**, 1506–1518.
- Katritch, V., Olson, W.K., Vologodskii, A., Dubochet, J. and Stasiak, A. (2000) Tightness of random knotting. *Phys. Rev. E. Stat. Phys.*, **61**, 5545–5549.
- Shaw, S.Y. and Wang, J.C. (1993) Knotting of a DNA chain during ring closure. *Science*, **260**, 533–536.
- Rybenkov, V.V., Cozzarelli, N.R. and Vologodskii, A.V. (1993) Probability of DNA knotting and the effective diameter of the DNA double helix. *Proc. Natl Acad. Sci. USA*, **90**, 5307–5311.
- Marenduzzo, D., Orlandini, E., Stasiak, A., Sumners, D., Tubiana, L. and Micheletti, C. (2009) DNA-DNA interactions in bacteriophage capsids are responsible for the observed DNA knotting. *Proc. Natl Acad. Sci. USA*, **106**, 22269–22274.
- Marenduzzo, D., Micheletti, C. and Orlandini, E. (2010) Biopolymer organization upon confinement. *J. Phys. Condens. Matter*, **22**, 283102.
- Stanley, C.B., Hong, H. and Strey, H.H. (2005) DNA cholesteric pitch as a function of density and ionic strength. *Biophys. J.*, **89**, 2552–2557.
- Lin, S., Numasawa, N., Nose, T. and Lin, J. (2007) Coarse-grained molecular dynamic simulations for lyotropic liquid-crystalline solutions of semiflexible rod-like molecules. *Mol. Cryst. Liq. Cryst.*, **466**, 53–76.
- Cifra, P., Benková, Z. and Bleha, T. (2008) Persistence lengths and structure factors of wormlike polymers under confinement. *J. Phys. Chem. B*, **112**, 1367–1375.
- Cifra, P. and Bleha, T. Shape transition of semi-flexible macromolecules confined in channel and cavity. *Eur. Phys. J. E.*, **32**, 273–279.
- Kron, A.K., Ptitsyn, O.B., Skvortsov, A.M. and Federov, A.K. (1967) A study of statistical globula-coil transition in macromolecules using the Monte-Carlo technique. *Molek. Biol.*, **1**, 576–582.

28. Reith,D. and Virnau,P. (2010) Implementation and performance analysis of bridging Monte Carlo moves for off-lattice single chain polymers in globular states. *Comput. Phys. Commun.*, **181**, 800–805.
29. Mansfield,M.L. (1994) Are there knots in proteins? *Nat. Struct. Biol.*, **1**, 213–214.
30. Virnau,P. (2010) Detection and visualization of physical knots in macromolecules. *Phys. Procedia*, **6**, 117–125.
31. Cifra,P., Benková,Z. and Bleha,T. (2008) Persistence lengths and structure factors of wormlike polymers under confinement. *J. Phys. Chem. B*, **112**, 1367–1375.
32. Trigueros,S. and Roca,J. (2007) Production of highly knotted DNA by means of cosmid circularization inside phage capsids. *BMC Biotechnol.*, **7**, 94.
33. Frisch,H.L. and Wasserman,E. (1961) Chemical topology. *J. Am. Chem. Soc.*, **83**, 3789–3795.
34. Delbrück,M. (1962) *Mathematical Problems in the Biological Sciences*, Vol. 14. Mathematical Society, Providence, Rhode Island, pp. 55–63.
35. Frank-Kamenetskii,M.D., Lukashin,A.V. and Vologodskii,A.V. (1975) Statistical mechanics and topology of polymer chains. *Nature*, **258**, 398–402.
36. Matthews,R., Louis,A.A. and Yeomans,J.M. (2009) Knot-controlled ejection of a polymer from a virus capsid. *Phys. Rev. Lett.*, **102**, 088101.
37. Marcone,B., Orlandini,E., Stella,A.L. and Zonta,F. (2007) Size of knots in ring polymers. *Phys. Rev. E Stat. Nonlin. Soft Matter Phys.*, **75**, 041105.
38. Virnau,P., Kantor,Y. and Kardar,M. (2005) Knots in globule and coil phases of a model polyethylene. *J. Am. Chem. Soc.*, **127**, 15102–15106.
39. Virnau,P., Mirny,L.A. and Kardar,M. (2006) Intricate knots in proteins: Function and evolution. *PLoS Comput. Biol.*, **2**, e122.
40. Ricca,R.L. (1998) New developments in topological fluid mechanics: from Kelvin's vortex knots to magnetic knots. In: Stasiak,A., Katritch,V. and Kauffman,L.H. (eds), *Ideal Knots*, Vol. 19. World Scientific, Singapore, pp. 255–273.
41. Micheletti,C., Marenduzzo,D., Orlandini,E. and Sumners,D.W. (2008) Simulations of knotting in confined circular DNA. *Biophys. J.*, **95**, 3591–3599.
42. Arsuaga,J. and Diao,Y. (2008) DNA knotting in spooling like configurations in bacteriophages. *Comp. Math. Methods Med.*, **9**, 303–316.